Supporting Information

New Generation of Mesoporous Silica Membranes Prepared by a Stöber-Solution Pore-Growth Approach

Marie-Alix Pizzoccaro-Zilamy[†], Cindy Huiskes[†], Enrico G. Keim[ł], Soraya Nicole Sluijter[‡], Henk van Veen[‡], Arian Nijmeijer[†], Louis Winnubst [†], and Mieke W.J. Luiten-Olieman[†]*

[†]Inorganic Membranes, MESA$^+$ Institute for Nanotechnology, University of Twente, P. O. Box 217, 7500 AE Enschede, The Netherlands

ł MESA$^+$ NanoLab, MESA$^+$ Institute for Nanotechnology, University of Twente, P. O. Box 217, 7500 AE Enschede, The Netherlands

‡ Sustainable Process Technology group, TNO, unit ECN part of TNO, P.O. Box 15, 1755 ZG Petten, The Netherlands

*m.d.pizzoccaro@utwente.nl

1. Schematic illustration for the Stöber-solution pore-growth synthesis

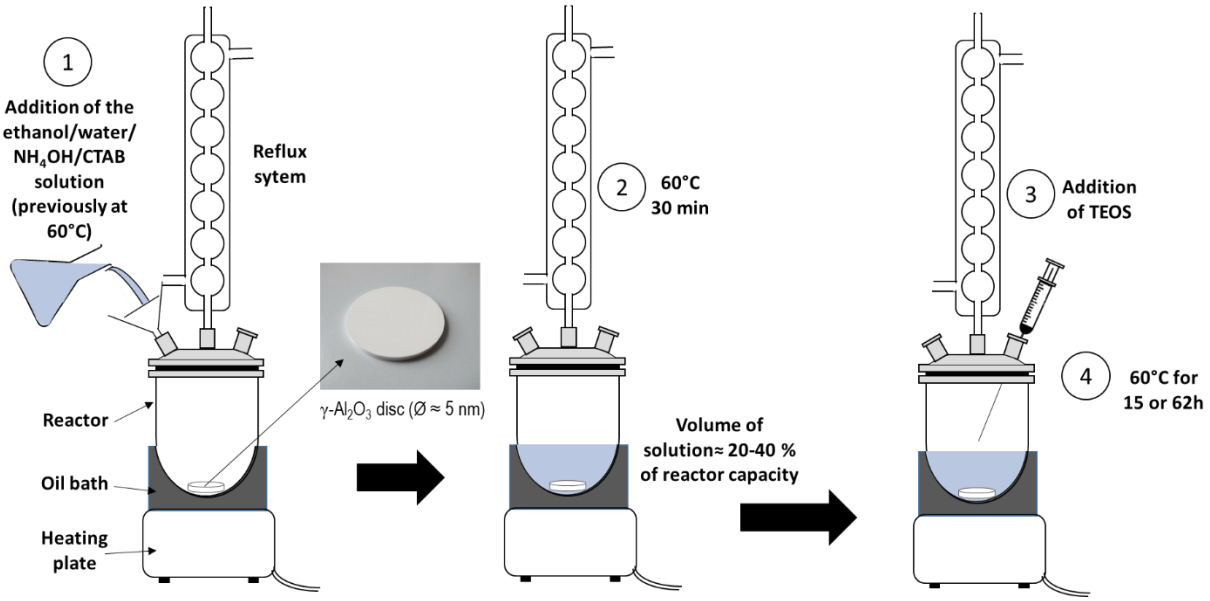

Figure S1. Schematic illustration for the Stöber-solution pore-growth synthesis.

2. SEM and permporometry analysis of MSM-EISA

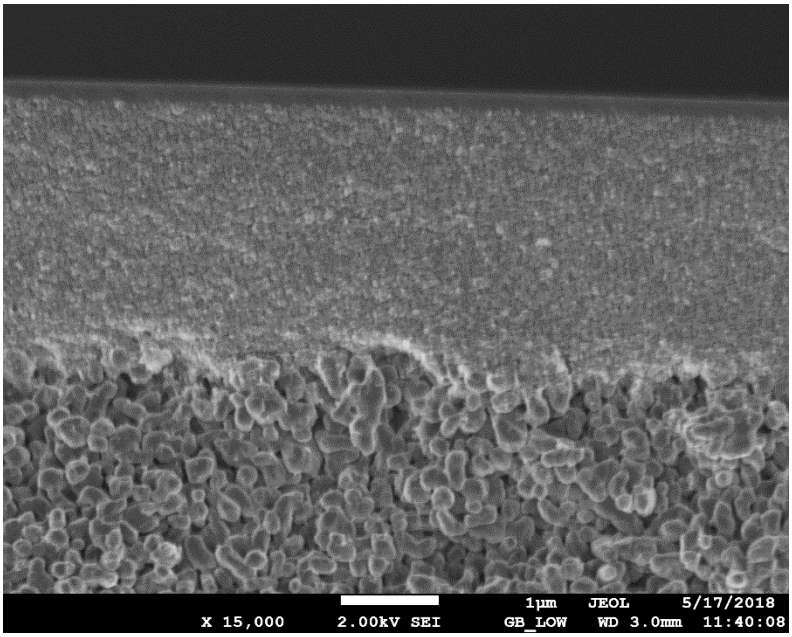

Figure S2. Cross-sectional FE-SEM image of the MSM-EISA sample.

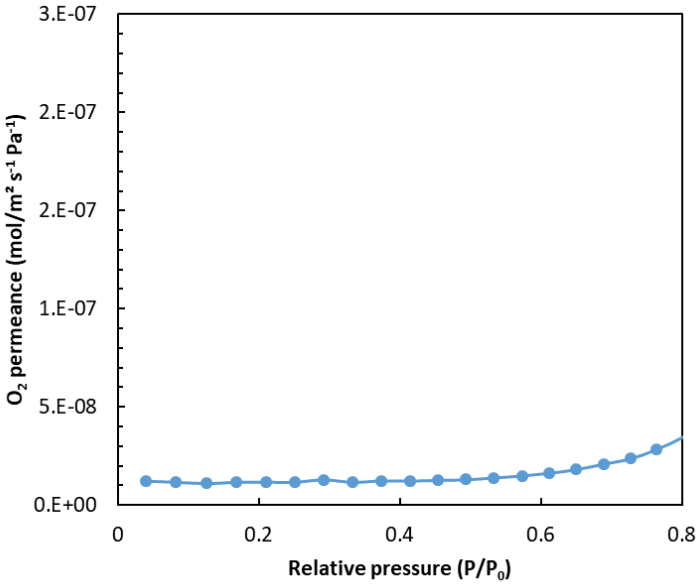

Figure S3. Oxygen flux vs. relative vapor pressure of cyclohexane for the MSM-EISA sample.

A constant oxygen permeance of 1×10^{-8} mol/(s m^2 Pa) was measured during the experiments. This value correspond to the detection limit of the experiment, and suggest thus that the O_2 permeance of the membrane is below 1×10^{-8} mol/(s m^2 Pa). The absence of clear transition point in this cyclohexane permporometry curve suggests thus the presence of micropores (pore diameter < 2 nm).

3. Top-surface SEM pictures of the sample MSM-B62

Figure S4. Top-surface FE-SEM images of the mesoporous silica membrane MSM-B62.

4. EDX analysis

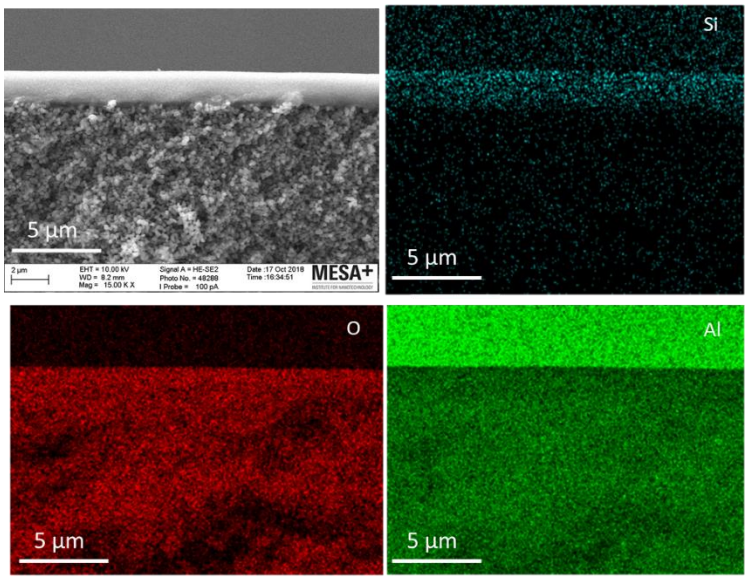

Figure S5. Cross-sectional FE-SEM image of the mesoporous silica membrane MSM-A15 and the corresponding EDXS maps.

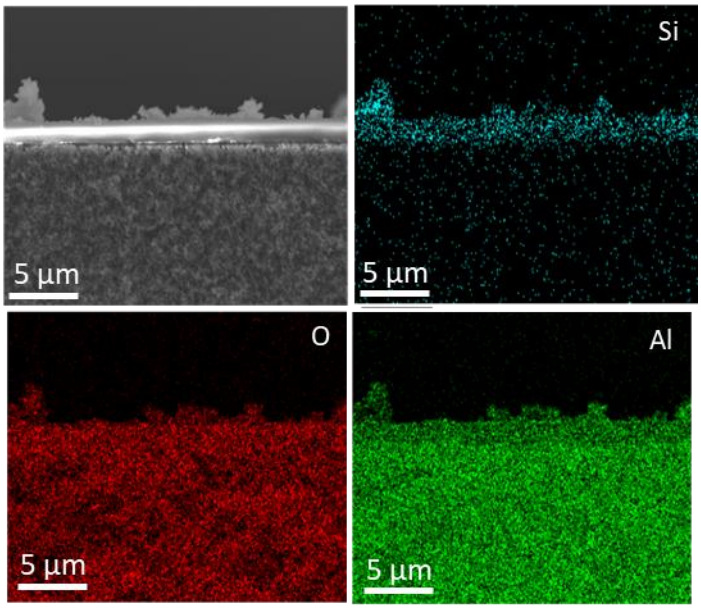

Figure S6. Cross-sectional FE-SEM image of the mesoporous silica membrane MSM-B15 and the corresponding EDXS maps.

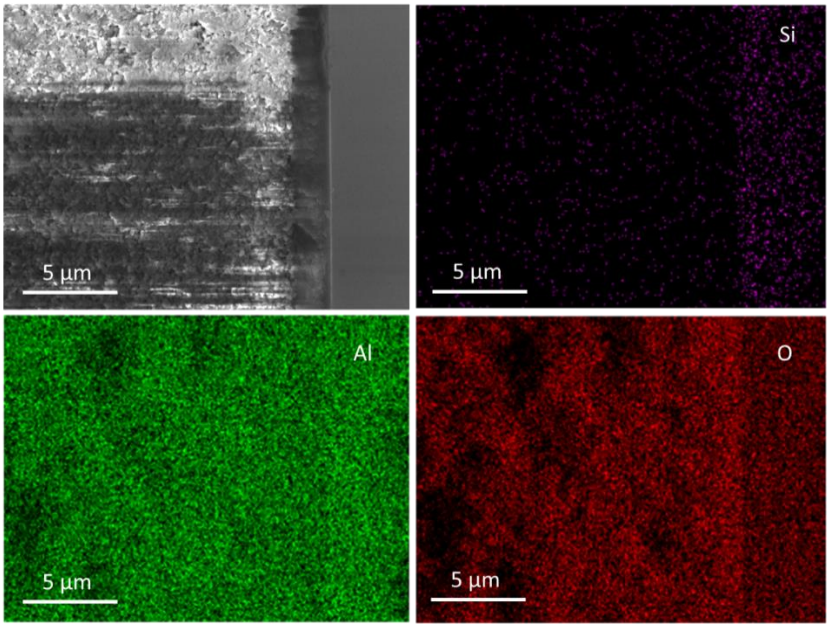

Figure S7. Cross-sectional FE-SEM image of the γ-Al_2O_3 support and the corresponding EDXS maps.

5. STEM-in-a-SEM analysis of the particles in the sol as function of the reaction time

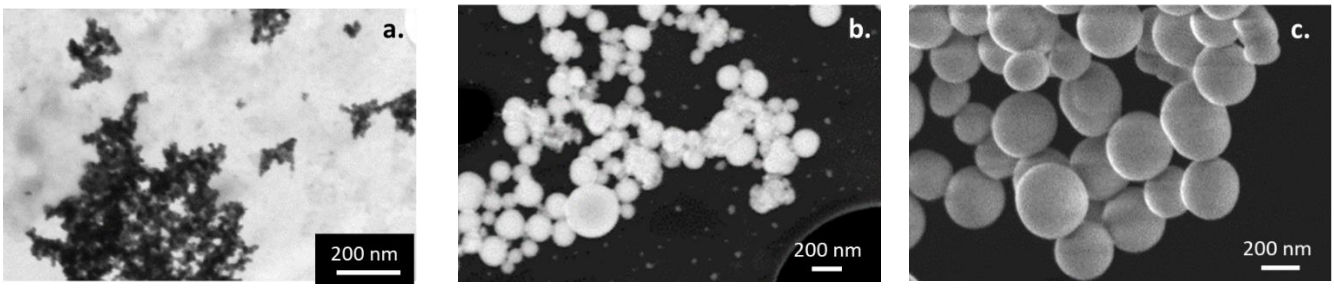

Figure S8. STEM-in-a-SEM pictures of the sol particles after reaction for 45 min (a.), 6h (b.) and 24h (c.).

6. Permporometry analysis

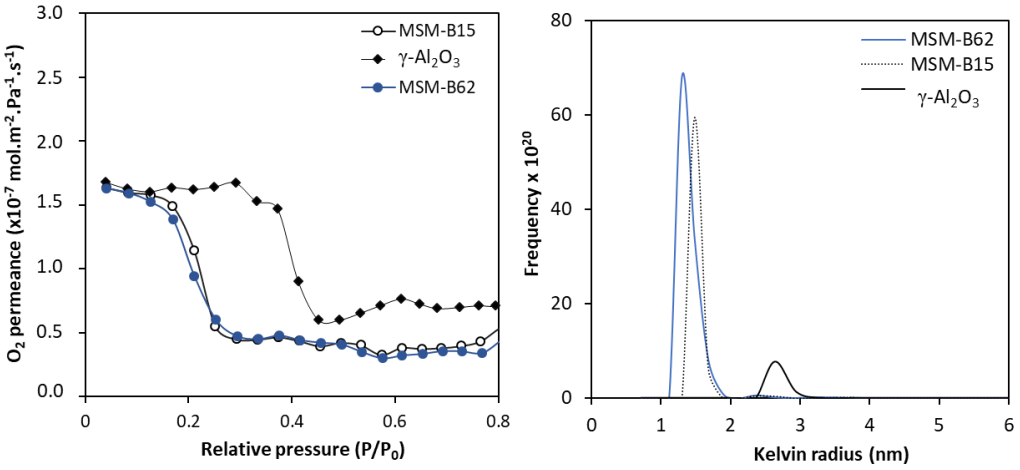

Figure S9. On the right Oxygen flux vs. relative vapor pressure of cyclohexane, on the left the pore size distribution for the mesoporous silica membranes and the pristine γ-Al_2O_3 support.

7. MWCO measurements

The composition of the feed, permeate and retentate (obtained at 30% of recovery) was analyzed by gel permeation chromatography (GPC). The GPC setup consisted of two PSS SUPREMA columns: 1000 Å, 10 µm, 8x300 mm and 30 Å, 10 µm, 8x300 mm columns from PSS Polymer Standards Service GmbH (Germany), a HPLC pump from Agilent 1200 series modules. The columns were calibrated using 16 different PEG standards (Mw: 62 – 42,000 g·mol^{-1}, PSS Polymer Standards Service GmbH, Germany). The GPC eluent consisted of pure water (MQ) containing 50 mg/L NaN_3. For each GPC analysis, 100 µL of a sample was injected into the GPC, which ran at 1 mL/min. Every GPC measurement was performed at least on two samples prepared under the same reaction conditions to ensure reproducibility. The rejection R was determined via Equation 1, where $C_{permeate}$ is the permeate concentration and C_{cell} the concentration inside the test cell. To correct for the inevitable accumulation of retained PEG molecules in a dead-end cell, the average of the original feed concentration and the final retentate concentration was used as C_{cell}.

$$R = 1 - \frac{C_{permeate}}{C_{cell}} \quad (1)$$

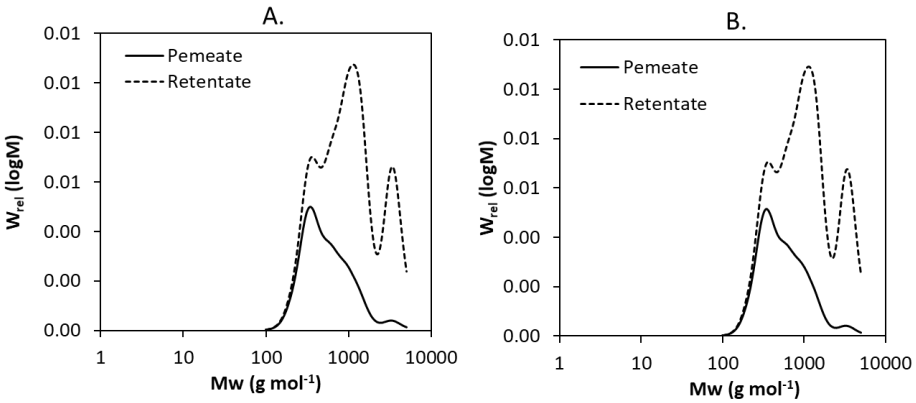

Figure S10. Molecular weight distribution of permeate and retentate for the membranes: A. MSM-B15, B. MSM-B62.

Table S1. Hydrodynamic diameters (d_H) of various polyethylene glycol and the experimental rejection values obtained for the MSMs at a pressure of 10 bar in water.

			MSM-B15	MSM-B62
Solute	Mw (g/mol)	d_H (nm)	R(%)	R(%)
PEG-300	300	0.8	26	21
PEG-600	600	1.18	56	60
PEG-1000	1000	1.57	77	78
PEG-1500	1500	1.97	86	86
PEG-3400	3400	3.1	94	95
Permeate Flux (L m^{-2} h^{-1})			17.7 ± 5.4	17.7 ± 1.1

8. Low angle XRD analysis of the sample MSM-B62

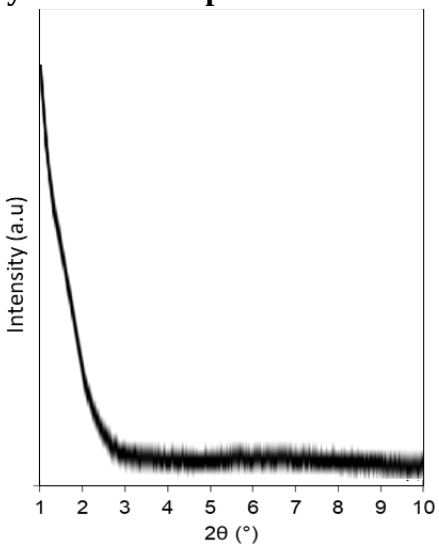

Figure S11. Low-angle XRD analysis for the mesoporous silica membrane MSM-B62.

9. GISAXS analysis of the sample MSM-B62

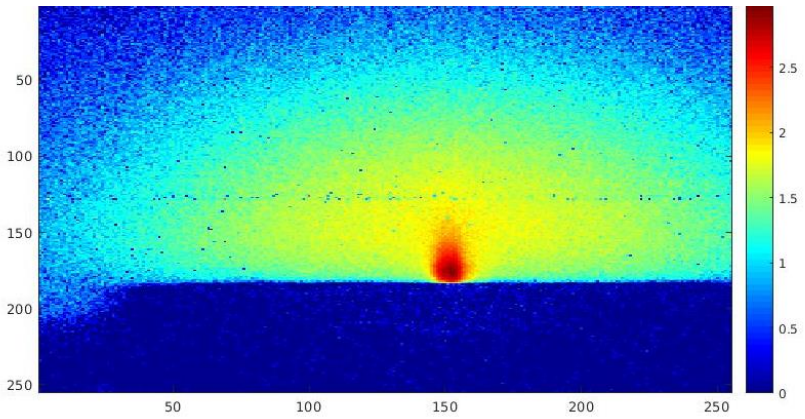

Figure S12. 2D-GISAXS scattering profiles of the mesoporous silica membrane MSM-B62.

10. Water flux vs. measurement time

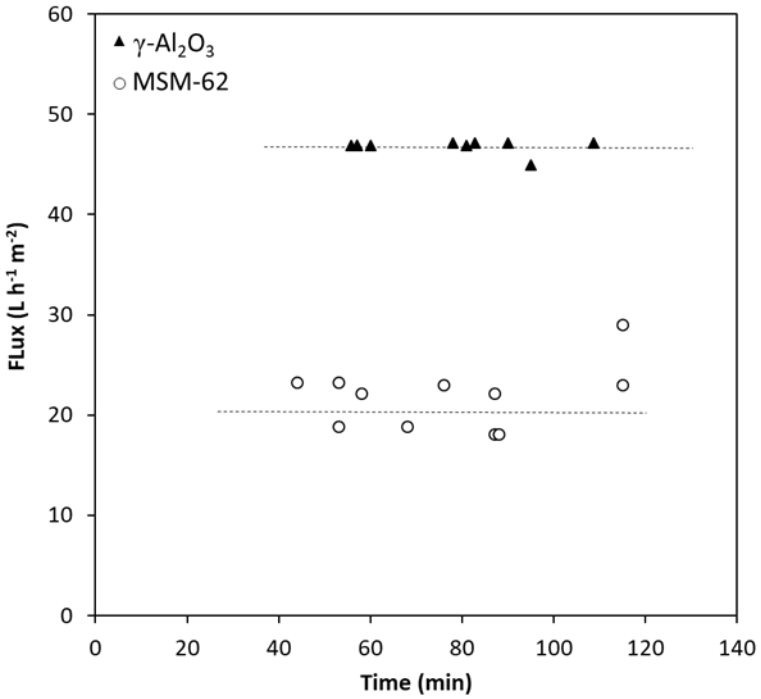

Figure S13. Water flux vs. measurement time through the pristine γ-Al_2O_3 support and the MSM-B62 membrane at a constant applied pressure of 8 bar. Drawn lines serve as guide to the eye.

11. Water flux by the viscosity vs. applied pressure

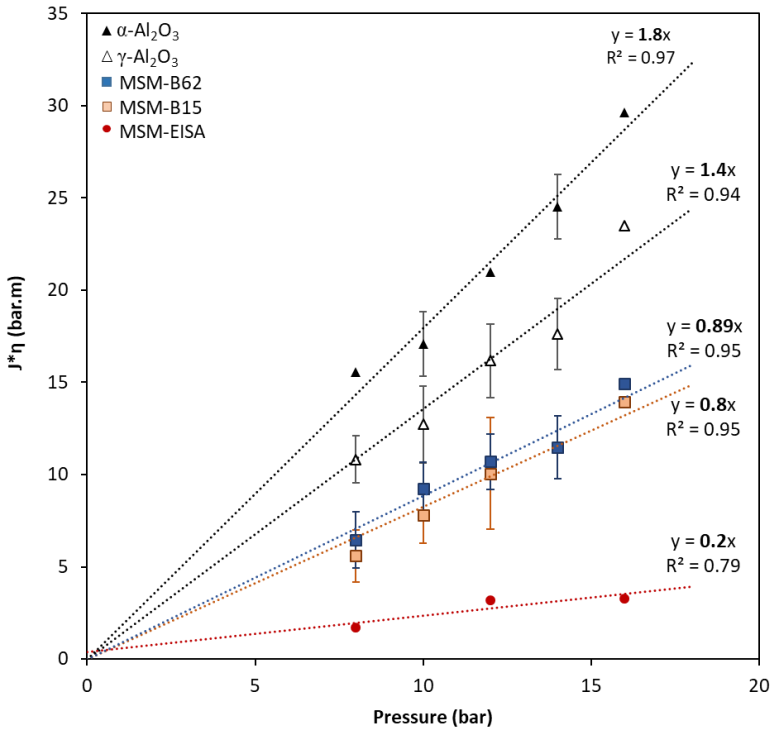

Figure S14. Viscosity corrected water flux vs. applied pressure for the α-Al_2O_3 and γ-Al_2O_3 pristine supports, and the mesoporous silica membranes (MSM-B15, MSM-B62 and MSM-EISA).

12. Water contact angle measurements

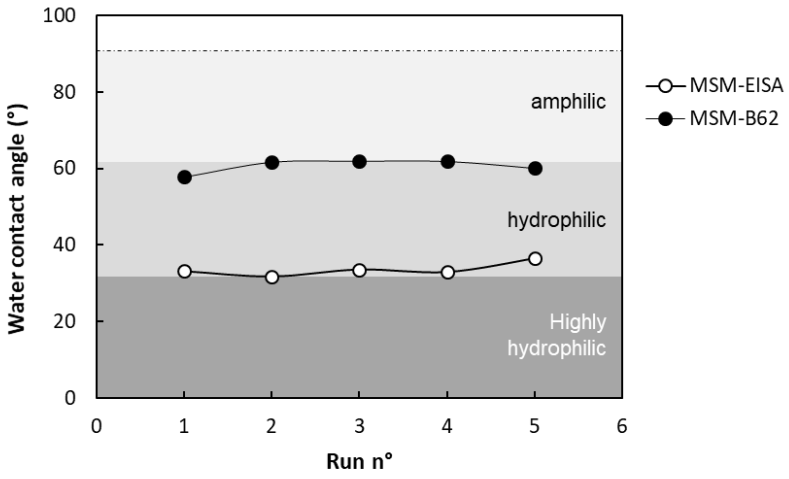

Figure S15. Water contact measurements of the mesoporous silica membranes: MSM-EISA and MSM-B62.